Carbon Fiber Production from Electrospun Sulfur Free Softwood Lignin Precursors

Samira Aslanzadeh, Behzad Ahvazi, Yaman Boluk, Cagri Ayranci

University of Alberta, Mechanical Engineering Department, Edmonton, Alberta, CANADA

Correspondence to:
Cagri Ayranci email: cayranci@ualberta.ca

ABSTRACT
In this study, a sulfur-free softwood lignin (SFSL) was electrospun to form bead-free fibers. The fibers were evaluated as potential precursors for carbon fiber production. Higher heating rates of thermo-stabilization caused afused fiber morphology. The lignin purification process also affected the quality of the SFSL-based carbon fibers. Therefore, the yield, morphological characteristics, structural characteristics, electrical conductivity and mechanical properties of the carbon fibers were evaluated. At higher carbonization temperatures crystalline carbon fibers were formed. As a result, as the carbonization temperature increased, the conductivity of SFSL-based carbon fibers also increased.

Keywords: Carbon fiber**,** lignin precursor, electrospinning, carbonization

INTRODUCTION
Carbon fibers are widely used to produce advanced reinforced composite materials with very high specific stiffness and strength properties.

Polyacrylonitrile (PAN) and petroleum pitch are the most commonly used precursor materials for producing carbon fibers. Although pitch based fibers provide higher modulus carbon fibers, they have a relatively small proportion of the market compared to PAN based fibers. Despite this, PAN-based fibers can provide higher tensile strength. Pitch-based carbon fibers are classified into two categories: isotropic pitch and anisotropic (mesophase) pitch. The isotopic carbon fibers (general purpose (GP) carbon fibers), produced from isotropic pitch, have the lowest moduli among carbon fibers [1, 2].The mesophase pitch-based fibers are considered high performance (HP) carbon fibers due to their high and ultra-high moduli and because the carbon layers are parallel to the fiber axis.

Due to processing costs, carbon fibers based on mesophase pitch are the most costly, isotropic pitch are the least costly, with the cost of PAN-based carbon fibers falls between the two [2]. The PAN precursors, however, account for approximately half the production costs and, as a result, PAN-based carbon fibers are prohibitively expensive for key industries with high production rates, such as the automotive and construction industries (33 $/Kg) [1].

Investigating alternative, low-cost precursors, like lignin, to reduce the cost of carbon fibers is a priority for many research groups [3-14]. Lignin is a biopolymer that has a three-dimensional amorphous structure. The formation of this biopolymer requires an enzyme and is initiated by dehydrogenative polymerization of the three different phenylpropane units. These units are linked by several different types of bonds resulting in a branched structure. After cellulose, lignin is the second most abundant biopolymer and the most plentiful aromatic (phenolic) natural macromolecule [15, 16] and chemical pulp plants produce large amounts of lignin every year as a by-product. However, the mechanical properties of lignin-based carbon fibers are less robust than those of typical commercial PAN-based carbon fibers. Thus, lignin-based carbon fibers are suitable only for general purposes [1]. Significant research efforts have been made to create value-added products from lignin, such as phenolic resins, epoxies, adhesive [17] and carbon fibers.

Carbon fiber production consists of three major steps: fiber spinning, thermo-stabilization and carbonization (pyrolization). There are also different spinning methods for the production of fibers: dry, wet, melt and electro spinning [13]. Electrospinning allows the formation of small-diameter fibers (micro- to nano-meter in diameter) that increase the surface-area-to-volume ratio of the end product and industry and researchers are giving the method increased attention [19].

A variety of research groups have studied the electrospinning of lignin [20-25]. These studies clearly illustrated that, in order to obtain smooth electrospun fibers, it is necessary to add poly(ethylene oxide) (PEO) to the lignin suspension [20-25]. The elasticity of the lignin suspension increased with increasing PEO concentration, when the molecular weight of PEO was unchanged. [24]. This was determined by calculating the relaxation time and Deborah (De) number [24]. The effects of PEO concentration and molecular weight on the morphology of the electrospun fibers (beaded fibers or bead free fibers) have been investigated [25]. Lignin macromolecules were characterized as a suspension of Brownian-collapsed rigid spherical particles in dimethylformamide (DMF), rather than a polymer solution with extended chains [24].

Carbon fiber production from electrospun lignin fibers has also been investigated [3-9], with different sources of lignin as a precursor for carbon fiber production were studied: softwood Kraft lignin [3-5], organosolv lignin [6-8] and alkali lignin [9]. Lignin electrospun carbon fibers can potentially be used in electrochemical capacitors [26] and anode materials for lithium ion batteries [8, 14].

Sulfur-free lignins are obtained from new biorefinery processes, which are expected to bring economic value to lignin [27]. In our previous work, we investigated the electrospinning of sulfur-free Softwood lignin (SFSL) [24, 25]. In this study, we report on the carbon fibers produced using the SFSL as a precursor. First, we show that different processes for purifying the SFSL affect the quality of carbon fibers and secondly, we investigate the properties of SFSL-based carbon fibers.

EXPERIMENTAL SECTION

Raw Materials

Two different types of Sulfur-free Softwood Lignin (SFSL), named L1 and L2, were used in this study. Alberta Innovates Technology Futures (AITF), Edmonton, AB, Canada provided the SFSL samples (Note: AITF has changed its name to InnoTech Alberta during the preparation of this manuscript, but the authors kept the name AITF in this paper). L1 and L2 were extracted from pin chips softwood furnishes received from a Kraft pulp mill (West Fraser Hinton kraft pulp mill), using AITF's proprietary lignin extraction and purification processes. The extraction and recovery processes were carried out under conventional chemical pulping conditions. These processes were further modified by employing proprietary methods. However, the purification step is a novel and a facile technique that was developed exclusively for preparing lignin as a precursor in formulation of carbon fibers. The constituents of the SFSL, based on AITF's information, are summarized in the *Table I*.

TABLE I. SFSL contents and specification.

Parameter		L1	L2
Solids	%	95	98.23
Composition based on bone dry material			
Lignin	%	97.2	97.66
Acid Insoluble Lignin	%	92.6	94.21
Acid Soluble Lignin	%	4.57	3.45
Ash	%	0.87	0.09
Hemicellulose Sugars	%	1.94	2.25

Poly(ethylene oxide) (PEO), with a molecular weight, M_v of 1,000 kD, was purchased from Sigma Aldrich and used in small amounts to aid in the electrospinning process. Molecular Biology Grade anhydrous N,N-dimethylformamide (DMF) was purchased from Sigma Aldrich and used as a solvent for SFSL/PEO electrospinning solutions.

Lignin Characterization

The molecular weights of SFSL (L1 and L2) were measured using Matrix-assisted laser desorption/ionization (MALDI) Mass Spectroscopy [24, 28], as summarized in *Table II*.

TABLE II. Calculated Mn and Mw based on MALDI spectrometry.

SFSL	Mw (Da)	Mn (Da)
L1 [24]	3823.3	2781.4
L2	3729.4	2688.3

To obtain the chemical composition of the specimens, XPS measurements were performed on an AXIS 165 spectrometer (Kratos Analytical). The base pressure in the analytical chamber was lower than 3×10^{-8} Pa. Monochromatic Al Kα source ($h\nu$ = 1486.6 eV) was used at a power of 168 W. The analysis spot was 400 x 700 um. The resolution of the instrument was 0.55 eV for Ag 3d and 0.70 eV for Au 4f peaks. The survey scans were collected for binding energy spanning from 1100 eV to 0 with analyzer pass

energy of 160 eV and a step of 0.4 eV. For the high-resolution spectra the pass-energy was 20 eV with a step of 0.1 eV. An electron flood gun was used to compensate the charging of the sample. Vision-2 instrument software was used to process the data. The spectra were calibrated for C1s binding energy position at 284.8 eV. Compositions were calculated from the survey spectra using the Shirley background and sensitivity factors provided by the instrument database. *Table* III shows mineral impurities in SFSL powders calculated based on the XPS results.

TABLE III. Ratio of mineral elements to carbon element in SFSL, obtained by XPS.

Ratio of mineral elements to carbon element	L1	L2
Na	0.0022	0.0013
S	0.0021	0.0009
Ca	0.005	0
Si	0.0657	0

Preparation of Spinning Solutions and Electrospinning

Electrospinning solutions were prepared as previously described [24, 25]. One series of SFSL + PEO (total solid (PEO/SFSL) concentration of 30 wt % in PEO/SFSL/DMF suspension, with PEO/SFSL ratio of 1/99) was investigated. This set was chosen as it provided the smooth (bead free) fibers with minimum aid of PEO [24, 25]. For the rest of the manuscript, it should be noted that the content of PEO in the lignin fibers was always 1wt %.

The horizontal electrospinning setup consisted of a syringe pump (GENEQ INC) with a blunt-tip 20 G needle. A high-voltage supply (GAMMA High Voltage), and a stationary collector with a constant working distance (tip-to-collector distance) of 0.2 m were used. The flow rate of 4.2×10^{-10} m^3 s^{-1} was supplied with a syringe pump. The applied voltage/distance ratio (electric field) was 70×10^3 V/m. The average diameter of SFSL electrospun fibers (prior to thermo-stabilization and carbonization) was 809 ± 26 nm and confidence limits calculated using a t-test [24].

Thermo-stabilization and Carbonization

The electrospun SFSL mats were placed horizontally in a combustion boat inside a furnace (LINDERBERG/BLUE). Thermo-stabilization was performed at various heating rates (0.5, 1 and 5°C/min) and at a constant thermo-stabilization temperature of 250ºC under atmospheric pressure and held for 60 min isothermally, as shown in *Table IV*.

TABLE IV. The thermo-stabilization conditions of SFSL.

Sample	Heating Rate (ºC/min)	Morphology
L1/PEO	5	Burnt Film
	1	Fused Fiber
	0.5	Fiber
L2/PEO	5	Burnt Film
	1	Extremely Fused Fiber
	0.5	Fused Fiber

The thermo-stabilized fiber mats were later placed in a combustion boat inside the furnace that had been purged with Argon. Carbonization was performed under an Argon flow at heating rate of 5 °C/min to 600, 750 and 900ºC and held for 60 min isothermally.

Characterization

The fibers were examined for their geometrical and morphological properties using a Hitachi S 4800 Field Emission scanning electron microscope (SEM) using gold-coated samples and an accelerating voltage of 20 kV.

Raman spectra were collected on a Nicolet Alimega XR Disposive Raman using a 50X microscope objective. The radiation was generated with a 532 nm Nd-Yag laser at 25% laser power (6 mW).

An x-ray diffraction (XRD) analysis was carried out with a Bruker D8-Discover. The X-ray beam was nickel-filtered CuKα radiation of wavelength 1.5406 Å, operated at 40 kV and 40 mA. Diffraction spectra were obtained over a 2θ - range of 10–60°C at a scanning rate of 0.02°C/s.

The electrical conductivities were measured by the four-point probe method (LUCAS LAB Pro4).

The mechanical properties of the carbonized fibers were measured by a tensile material testing system (ElectroForce 3200 Series III, Bose Corporation, USA) equipped with a 250 g load cell. The electrospun mats (length of 5 cm and width of 0.5 cm) were mounted on paper sample holders. The gage length and the extension rate were 3 cm and 0.01 mm/s, respectively.

RESULTS AND DISCUSSION

Thermo-stabilization of SFSL Electrospun Fibers

We have discussed the formation of the lignin fibers using electrospinning in our previous works [24, 25]. *Table IV* summarizes the morphology of the electrospun lignin fibers. As can be seen, the morphology depends highly on the heating rate of the thermo-stabilization. Both L1 and L2 electrospun fibers turned into burnt films and fused fibers when heating rates were higher than 0.5ºC/min. L1 electrospun fibers were successfully thermo-stabilized and uniform fibers were formed at the heating rate of 0.5ºC/min, but again L2 electrospun fibers formed fused fibers at this heating rate.

The SEM images of L1 and L2 in *Figure 1* show thermo-stabilized fibers with the heating rate of 1ºC/min. Fibers do not maintain their shapes at this heating rate, but are fused and stuck together, as seen from this figure and outlined in *Table IV*. The L2 fibers were more severely fused than the L1 fibers.

The non-fused, thermo-stabilized L1 electro-spun fibers were achieved with the heating rate of 0.5ºC/min. However, there was still some partial fusion in L2 electro-spun fibers at this heating rate, as shown in *Figure 2*.

During thermo-stabilization, lignin is subjected two thermally-induced mechanisms [20]: (1) an increase in mobility because of temperature-induced polymer relaxations; and (2) a decrease in mobility because of high temperature cross-linking.

A faster heating rate generally leads to relaxation instead of cross-linking; as a result, higher flow occurs resulting in fused fibers. With slower heating rates cross-linking occurs before relaxation, causing increasing Tg and lower polymer flow, resulting in less fiber fusion [20, 29].

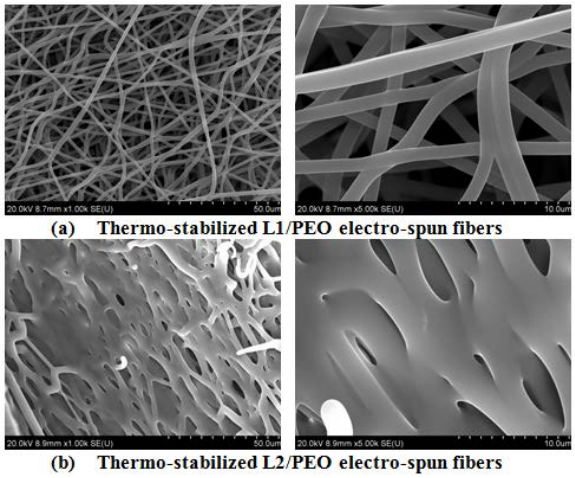

FIGURE 1. SEM images of thermo-stabilized (a) L1/PEO and (b) L2/PEO electro-spun fibers. The heating rate was 1ºC/min from room temperature to 250ºC and holding isothermally 1 h in air atomosphere. (left and right image scales are 50 and 10 micrometers, respectively).

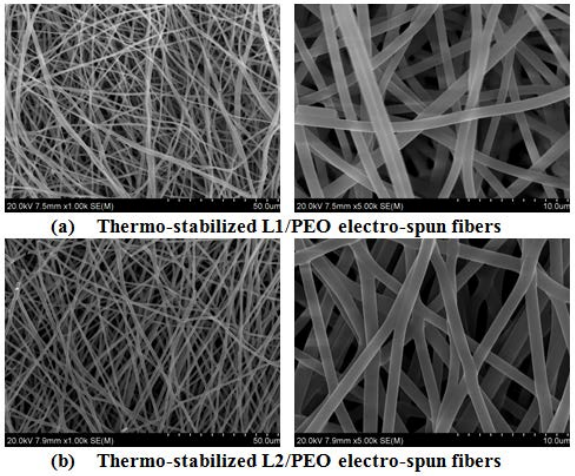

FIGURE 2. SEM images of thermo-stabilized (a) L1/PEO and (b) L2/PEO electro-spun fibers. The heating rate is 0.5ºC/min from room temperature to 250ºC and holding isothermally 1 h in air atomosphere. (left and right image scales are 50 and 10 micrometers, respectively).

By comparing the morphology of thermo-stabilized fibers, one can conclude that L1 has lower thermal mobility than that of L2 which causes the fibers to fuse much less than that of L2.

Fiber fusion is a defect, which is not desired during carbon fiber production. In the literature [20, 29], the formation of fused fibers and burnt films was attributed to lower molecular fraction of lignin. However, here the Mw and polydispersity of L1 and L2 are almost the same. Additionally, the hemicellulose content of L1 was less than that of L2. The hemicellulose content may affect the thermal mobility of SFSL during thermo-stabilization process. This should be investigated further in the future.

Carbonization and Characterization of Carbonized SFSL Electrospun Fibers

Figure 3 shows the morphology of SFSL thermo-stabilized fibers after the carbonization process at 900ºC. The non-fused L1 carbon fibers can be achieved from non-fused L1 thermo-stabilized fibers (corresponding to *Figure 2*). However, L2 material was not used for the remainder of the study because, under these same conditions, L2 carbon fibers fused.

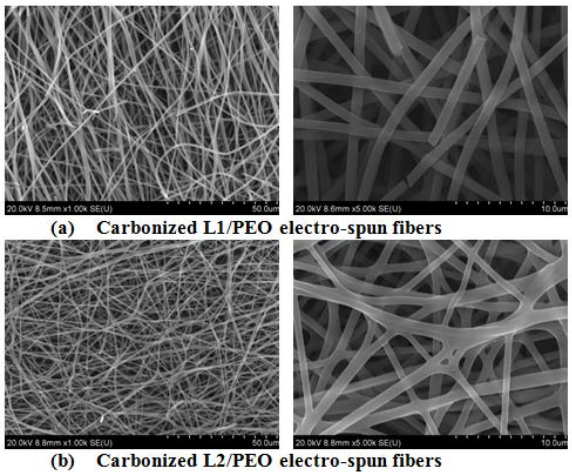

FIGURE 3. SEM images of carbonized (a) L1/PEO and (b) L2/PEO electro-spun fibers. The heating rate is 0.5ºC/min from room temperature to 250ºC and holding isothermally 1 h in air atmosphere, then the heating rate is 5ºC/min from 250ºC to 900ºC and holding isothermally 1 h in Argon atmosphere. (left and right image scales are 50 and 10 micrometers, respectively).

We characterized the carbon fibers according to five categories: weight loss, degree of graphitazitation, X-ray diffraction (XRD), conductivity, and mechanical properties.

Weight Loss

Figure 4 presents the weight loss of SFSL fibers when carbonized at different temperatures. The experiments showed 60%, 67% and 74% weight loss respectively when the fibers were carbonized at 600, 750, and 900°C. This suggests that higher weight loss occurs as the carbonization temperature is increased.

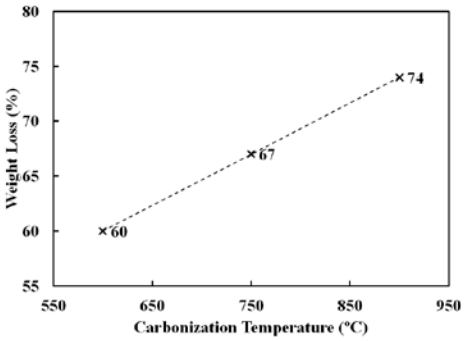

FIGURE 4. The weight loss of SFSL-based carbonized fibers (L1) as a function of carbonization temperature

According to the literature, [7, 10], on lignin-based carbonized fibers, the majority of weight loss occurs in the carbonization step due to loss of volatile products. The weight losses for hardwood Kraft lignin [10] and Alcell [7, 10] are reported around 55% and 60-65 % at $T_C = 1000℃$, respectively. Weight loss in our SFSL based carbon fiber was 74%. This dissimilarity is related to the chemical structure of lignin, which is not the same across all kind of lignins.

Degree of Graphitazitation

Figure 5 shows Raman spectra of SFSL-based carbonized fibers at different carbonization temperatures. The degree of graphitization is evaluated by the two main peaks occurring around 1580 (G-peak) and 1360 cm^{-1} (D-peak) in Raman spectra for most carbon-graphite products [31, 32]. However, natural graphite has a single sharp band at 1575-1580 cm^{-1} (G-peak)) [31, 33]. The G-peak and the D-peak are related to the graphite structure and graphitized carbon structure, respectively [31]. The D-peak is related to the disordered portion of carbons, while the G-peak is due to the ordered graphite crystallites of the carbons [34].

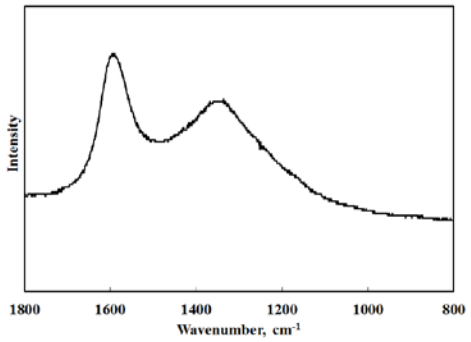

(a) Carbonization temperature of 600ºC

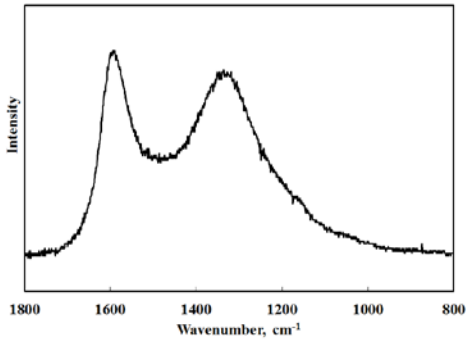

(b) Carbonization temperature of 750ºC

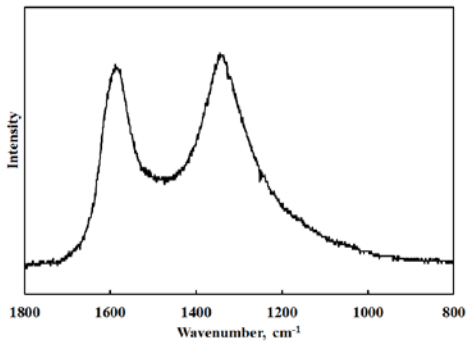

(c) Carbonization temperature of 900ºC

FIGURE 5. Raman spectra of SFSL -based carbonized fibers (L1).

Table V shows the peak positions (G-peak and D-peak) of SFSL-based carbonized fibers at different carbonization temperatures. In SFSL-based carbonized electrospun fibers, the G-peak is around 1589-1590 cm^{-1} and it stays constant by increasing the carbonization temperature (*Figure 5 (a), (b) and (c)*). The D-peak is around 1336 cm^{-1} at carbonization temperature of 600ºC and 750ºC. This increases to 1345 cm^{-1} at carbonization temperature of 900ºC.

TABLE V. G-peak and D-peak positions at different temperatures of carbonization.

Temperature of carbonization (ºC)	600	750	900
G-peak (cm^{-1})	1590	1590	1589
D-peak (cm^{-1})	1336	1336	1345

Figure 6 demonstrates the ratio of D-peak (I_D) to G-peak (I_G). This ratio was calculated based on the height (max point of the peak) and area (area under the peak curve) of the peaks (*Figure 6*). The degree of graphitization was evaluated by the ratio of D-peak (I_D) to G-peak (I_G) [32, 35]. This ratio, (I_D/I_G), increases with carbonization temperature in SFSL-based carbonized fibers. However, this is different from the results of PAN-based carbon fibers [4, 31, 36], for which the (I_D/I_G) ratio decreases with increasing carbonization temperature [4, 31, 34, 36, 37]. During the carbonization of PAN, the smaller I_D/I_G ratio indicates the higher degree of graphitization of carbon products [4, 31, 34, 36, 37].

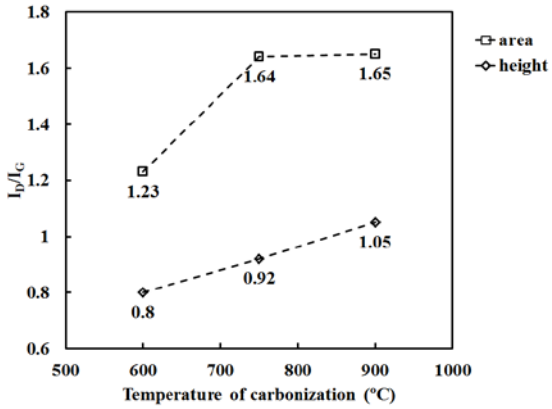

FIGURE 6. The ratio of D-peak to G-peak (I_D/I_G) of SFSL-based carbon fibers (L1). (I_D/I_G) calculated from Raman spectra based on height and area of peaks.

Dallmeyer et al. compared the results of Raman spectra for lignin- and PAN-based carbonized electrospun fibers [4]. They [4] illustrated that the (I_D/I_G) ratio for lignin-based carbonized fibers increases with the carbonization temperature, confirming our findings. However, this ratio for PAN-based carbonized fibers decreases within the same carbonization temperature ranges. The authors attribute this dissimilarity to the different structure of lignin and PAN [4, 38]. They also suggested from their results that lignin-based carbon fibers could be more amorphous at carbonization temperature of 600ºC.

However, by increasing the carbonization temperature to 800-1000ºC, these carbon fibers may transform from amorphous carbon to nano-crystalline graphite structures [4]. On the other hand, PAN fibers already have the nano-crystalline structure at 600ºC [4].

Before the carbonization process, lignin is an amorphous biopolymer as compared to PAN, which is a semi-crystalline polymer. During the carbonization of lignin, the ratio of the I_D/I_G increases as the transformation from an amorphous carbon to a nano-crystalline graphite occurs. This ratio increases due to nucleation, growth and clustering of aromatic rings in lignin [4].

We conclude that the formation of nano-crystalline graphite structure in lignin occurs at higher temperature of carbonization compared to that of PAN. Tenhaef et al, from Oak Ridge National Laboratory, carbonized the lignin at higher carbonization temperature (1000ºC, 1500ºC and 2000ºC) [14]. They reported [14] Raman spectra of lignin-based carbonized fibers at different carbonization temperatures. Numerical values were not reported for the (I_D/I_G) ratio of lignin-based carbonized fibers by Tenhaef et al [14]. Using their graphs, we calculated a decreased (I_D/I_G) ratio with increasing carbonization temperature. This ratio was around 0.9 for carbonization temperature of 1000ºC and 1500ºC, which is close to our ratio. However, the ratio decreased to 0.5 at a carbonization temperature of 2000ºC [14]. Therefore, a nano-crystalline graphite structure in lignin may be obtained at a carbonization temperature of 2000ºC.

X-ray Diffraction

We concluded that, at lower carbonization temperature, lignin has an amorphous carbon structure. This amorphous carbon structure transforms to nanocrystallite graphite at higher carbonization temperature [14].

Figure 7 shows the X-ray diffraction (XRD) pattern of the SFSL-based carbonized fibers at the carbonization temperature of 900ºC. In this pattern, there are two peaks at $2\theta \approx 26^\circ$ and $2\theta \approx 43^\circ$. These peaks correlates to the (002) and (100) reflections in the graphite structure [39].

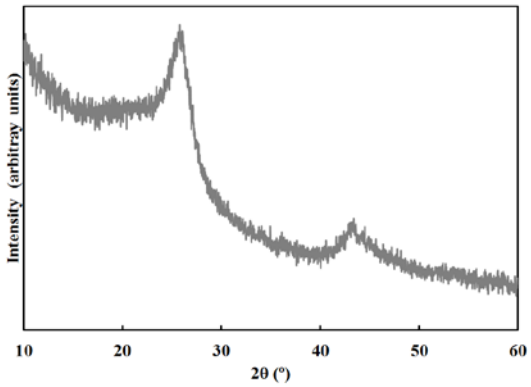

FIGURE 7. X-ray diffraction patterns of SFSL-based carbonized fibers (L1).

The average interlayer spacing d_{002} (d-spacing) was calculated by the Bragg equation [36] as follows:

$$\lambda = 2dsin\theta \quad (1)$$

where θ and λ are the scattering angle and wavelength of the X-ray, respectively.

According to equation 1, d_{002} was calculated as 0.345 nm for our case.

L_c and L_a are the lattice parameters (crystallite dimensions) along the c-axis and the a- axis, respectively [39]. The crystallite dimensions ($L_{c(002)}$ and $L_{a(100)}$) were obtained from Scherrer equations [36] as follows:

$$L_{c(002)} = 0.91\lambda/\beta cos\theta \quad (2)$$

$$L_{a(100)} = 1.84\lambda/\beta cos\theta \quad (3)$$

where β is the half maximum line width in radians. According to equations 2 and 3, L_c and L_a are calculated as 3.33 nm and 7.58 nm, respectively.

No XRD peaks were observed for carbonization temperatures of 600ºC and 750ºC. Therefore, at these carbonization temperatures, the SFSL-based carbonized fibers are amorphous carbon fibers.

Conductivity*:*

The electrical resistance (R) and resistivity (ρ) of SFSL-based carbonized fibers are summarized in the Table VI. Resistivity (ρ) was calculated as follows [36]:

$$\rho = \frac{R}{L} A \quad (4)$$

where A is the cross-section of the web. A was calculated by multiplying the measured width by the measured thickness of the sample web. L is the distance between 2 electrodes, 0.102 cm for our measurements [36].

TABLE VI. Electrical resistance and resistivity of SFSL-based carbonized fibers (L1).

Carbonization Temperature	Electrical Resistance (R)	R/L	Resistivity
(ºC)	(ohm)	(ohm/cm)	(ohm.cm)
900	61.9	606.8	0.4247
750	1038	10171	6
600	806,900,000	7,910,784,314	9,492,941

Figure 8 presents the electrical conductivity of the SFSL-based carbonized fibers as a function of carbonization temperature. Conductivity was calculated as follows:

$$\sigma = \frac{1}{\rho} \quad (5)$$

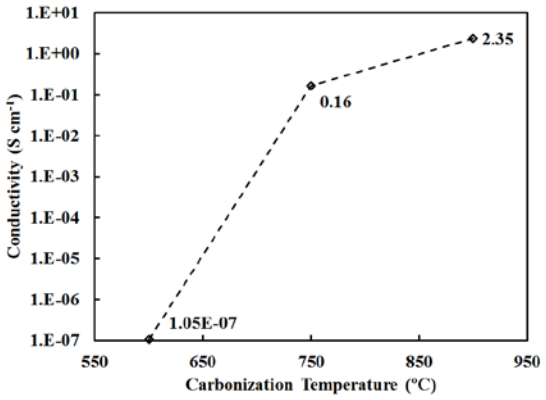

FIGURE 8. Electrical conductivity of SFSL-based carbonized fibers (L1) as a function of carbonization temperature.

Conductivity of electrospun carbon fibers increases with carbonization temperature, as shown in *Figure 8*. SFSL-based carbonized fibers have very low conductivity at $T_C = 600$ ℃. By increasing the carbonization temperature from 600 to 750ºC, the conductivity increases by ~6 orders of magnitude. With carbonization temperatures from 750 to 900ºC, the conductivity increases by one order of magnitude.

The increase in conductivity with the carbonization temperature agrees well with our X-ray diffraction results. Ordered crystals form when carbonization occurs at higher temperatures.

Mechanical Properties

Figure 9 shows the stress-strain curves of the SFSL-based carbonized fibers at a carbonization temperature of 900ºC. The average ultimate tensile strength experienced by the mats was 0.0085 ± 0.0045 N/Tex. Testing the samples was challenging due to the randomly distributed web structure of the carbon fibers which contributed to the large deviation in the results.

The tensile strength of Indulin-AT lignin-based carbonized fibers at a carbonization temperature of 1000ºC is reported as 32 ± 9 MPa (0.023 ± 0.007 N/Tex) [4]. The strength of Indulin-AT-based carbon fibers is 3 times more than that of SFSL-based carbonized fibers, since the Mw of fractionated lignin utilized for carbonization is around 35,000 Da [4]. In this research, we utilized unfractionated SFSL, with a molecular weight of around 3,800 Da. Further, SFSL lost 74% of its weight during carbonization, while this value was around 55% for Indulin-AT [10].

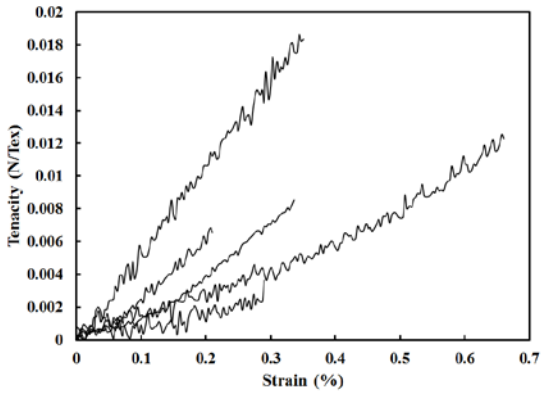

FIGURE 9. Typical stress–strain curves of SFSL-based carbonized fibers (L1) at a carbonization temperature of 900ºC.

CONCLUSION

In this work, SFSL-based fibers were prepared using electrospinning. These fibers were then thermo-stabilized and carbonized. The study showed that higher heating rates resulted in undesirable fused fiber morphology. Therefore, the thermo-stabilization process was carried out using a heating rate of 0.5 °C/min from room temperature to 250 °C. The specimens were kept at this temperature for 1 hour. The effects of the purification process are highlighted and discussed for the thermo-stabilized fibers.

An x-ray diffraction (XRD) analysis showed that at carbonization temperature of 600ºC and 750ºC amorphous carbon fibers were obtained. Crystalline carbon fibers were obtained by increasing the carbonization temperature to 900ºC.

The electrical conductivities of SFSL-based carbonized fibers are directly related to the carbonization temperature. By increasing carbonization temperature from 600 to 750ºC, the conductivity increases by 6 orders of magnitude and by one order of magnitude when the temperature was increased from 750 to 900ºC.

Raman spectroscopy results demonstrated that a nanocrystalline graphite structure was not obtained in SFSL-based carbonized fibers at the carbonization temperature of 900ºC. According to the literature [14], nanocrystalline graphite can be obtained at a carbonization temperature of 2000ºC. The formation of crystalline structure in lignin occurs at higher temperature of carbonization compared to PAN.

The average ultimate tensile strength of the carbonized fibers was 0.0085 ± 0.0045 N/Tex. More tests need to be done in order to decrease the spread in data.

ACKNOWLEDGEMENT

The authors would like to acknowledge funding provided by Alberta Innovates Bio-Solutions (Funding Number: ABI-14-001 / RES0022603) for the completion of this research project. Additionally, the authors would like to also acknowledge the in-kind support provided during this project by Alberta Innovates Technology Futures (AITF) and National Institute for Nanotechnology (NINT) in Edmonton, AB, Canada.

REFERENCES

[1] Park, S.-J., *Carbon fibers*. 2015: Springer.

[2] Chung, D., *Carbon fiber composites*. 2012: Butterworth-Heinemann.

[3] Lin, L., Y. Li, and F.K. Ko, *Fabrication and properties of lignin based carbon nanofiber.* Journal of Fiber Bioengineering and Informatics, 2013. 6(4): p. 335-347.

[4] Dallmeyer, I., et al., *Preparation and Characterization of Interconnected, Kraft Lignin-Based Carbon Fibrous Materials by Electrospinning.* Macromolecular Materials and Engineering, 2014. 299(5): p. 540-551.

[5] Goudarzi, A., L.-T. Lin, and F.K. Ko, *X-Ray Diffraction Analysis of Kraft Lignins and Lignin-Derived Carbon Nanofibers.* Journal of Nanotechnology in Engineering and Medicine, 2014. 5(2): p. 021006-021006.

[6] Lallave, M., et al., *Filled and hollow carbon nanofibers by coaxial electrospinning of alcell lignin without binder polymers.* ADVANCED MATERIALS-DEERFIELD BEACH THEN WEINHEIM-, 2007. 19(23): p. 4292.

[7] Ruiz-Rosas, R., et al., *The production of submicron diameter carbon fibers by the electrospinning of lignin.* Carbon, 2010. 48(3): p. 696-705.

[8] Wang, S.-X., et al., *Lignin-derived fused electrospun carbon fibrous mats as high performance anode materials for lithium ion batteries.* ACS applied materials & interfaces, 2013. 5(23): p. 12275-12282.

[9] Hu, S. and Y.-L. Hsieh, *Ultrafine microporous and mesoporous activated carbon fibers from alkali lignin.* Journal of Materials Chemistry A, 2013. 1(37): p. 11279-11288.

[10] Kadla, J.F., et al., *Lignin-based carbon fibers for composite fiber applications.* Carbon, 2002. 40(15): p. 2913-2920.

[11] Kubo, S. and J. Kadla, *Lignin-based carbon fibers: Effect of synthetic polymer blending on fiber properties.* Journal of Polymers and the Environment, 2005. 13(2): p. 97-105.

[12] Baker, D.A., N.C. Gallego, and F.S. Baker, *On the characterization and spinning of an organic-purified lignin toward the manufacture of low-cost carbon fiber.* Journal of Applied Polymer Science, 2012. 124(1): p. 227-234.

[13] Baker, D.A. and T.G. Rials, *Recent advances in low-cost carbon fiber manufacture from lignin.* Journal of Applied Polymer Science, 2013. 130(2): p. 713-728.

[14] Tenhaeff, W.E., et al., *Highly Robust Lithium Ion Battery Anodes from Lignin: An Abundant, Renewable, and Low-Cost Material.* Advanced Functional Materials, 2014. 24(1): p. 86-94.

[15] Suhas, P.J.M. Carrott, and M.M.L. Ribeiro Carrott, *Lignin – from natural adsorbent to activated carbon: A review.* Bioresource Technology, 2007. 98(12): p. 2301-2312.

[16] Chakar, F.S. and A.J. Ragauskas, *Review of current and future softwood kraft lignin process chemistry.* Industrial Crops and Products, 2004. 20(2): p. 131-141.

[17] Stewart, D., *Lignin as a base material for materials applications: Chemistry, application and economics.* Industrial crops and products, 2008. 27(2): p. 202-207.
[18] Reneker, D.H. and A.L. Yarin, *Electrospinning jets and polymer nanofibers.* Polymer, 2008. 49(10): p. 2387-2425.
[19] Thompson, C., et al., *Effects of parameters on nanofiber diameter determined from electrospinning model.* Polymer, 2007. 48(23): p. 6913-6922.
[20] Dallmeyer, I., S. Chowdhury, and J.F. Kadla, *Preparation and Characterization of Kraft Lignin-Based Moisture-Responsive Films with Reversible Shape-Change Capability.* Biomacromolecules, 2013. 14(7): p. 2354-2363.
[21] Dallmeyer, I., F. Ko, and J.F. Kadla, *Electrospinning of Technical Lignins for the Production of Fibrous Networks.* Journal of Wood Chemistry and Technology, 2010. 30(4): p. 315-329.
[22] Dallmeyer, I., F. Ko, and J.F. Kadla, *Correlation of Elongational Fluid Properties to Fiber Diameter in Electrospinning of Softwood Kraft Lignin Solutions.* Industrial & Engineering Chemistry Research, 2014. 53(7): p. 2697-2705.
[23] Poursorkhabi, V., A.K. Mohanty, and M. Misra, *Electrospinning of aqueous lignin/poly (ethylene oxide) complexes.* Journal of Applied Polymer Science, 2015. 132(2).
[24] Aslanzadeh, S., et al., *Electrospinning of Colloidal Lignin in Poly (ethylene oxide) N, N-Dimethylformamide Solutions.* Macromolecular Materials and Engineering, 2016.
[25] Aslanzadeh, S., et al., *Morphologies of Electrospun Fibers of Lignin in Poly(ethylene oxide) / N,N-Dimethylformamide* Journal of Applied Polymer Science, 2016.
[26] Inagaki, M., Y. Yang, and F. Kang, *Carbon nanofibers prepared via electrospinning.* Advanced Materials, 2012. 24(19): p. 2547-2566.
[27] Lora, J.H. and W.G. Glasser, *Recent industrial applications of lignin: a sustainable alternative to nonrenewable materials.* Journal of Polymers and the Environment, 2002. 10(1-2): p. 39-48.
[28] Kosyakov, D., et al., *Optimization of sample preparation conditions in the study of lignin by MALDI mass spectrometry.* Journal of Analytical Chemistry, 2014. 69(14): p. 1344-1350.
[29] Braun, J., K. Holtman, and J. Kadla, *Lignin-based carbon fibers: Oxidative thermostabilization of kraft lignin.* Carbon, 2005. 43(2): p. 385-394.
[30] Baker, D.A. and O. Hosseinaei, *High Glass Transition Lignins and Lignin Derivatives for the Manufacture of Carbon and Graphite Fibers*. 2014, Google Patents.
[31] Zou, L., et al., *An investigation of heterogeneity of the degree of graphitization in carbon–carbon composites.* Materials Chemistry and Physics, 2003. 82(3): p. 654-662.
[32] Yen, B., *An investigation of friction and wear mechanisms of carbon-carbon composites in nitrogen and air at elevated temperatures.* Carbon, 1996. 34(4): p. 489-498.
[33] Tuinstra, F. and J.L. Koenig, *Raman spectrum of graphite.* The Journal of Chemical Physics, 1970. 53(3): p. 1126-1130.
[34] Kim, C., et al., *Fabrication of Electrospinning-Derived Carbon Nanofiber Webs for the Anode Material of Lithium-Ion Secondary Batteries.* Advanced Functional Materials, 2006. 16(18): p. 2393-2397.Nakamizo, M., R. Kammereck, and P.L. Walker, *Laser Raman studies on carbons.* Carbon, 1974. 12(3): p. 259-267.
[35] Kim, C., et al., *Raman spectroscopic evaluation of polyacrylonitrile-based carbon nanofibers prepared by electrospinning.* Journal of Raman Spectroscopy, 2004. 35(11): p. 928-933.
[36] Park, S.H., C. Kim, and K.S. Yang, *Preparation of carbonized fiber web from electrospinning of isotropic pitch.* Synthetic metals, 2004. 143(2): p. 175-179.
[37] Davé, V., et al., *Molecular organization of lignin during carbonization.* Polymer, 1993. 34(15): p. 3144-3154.
[38] Babu, V.S. and M.S. Seehra, *Modeling of disorder and X-ray diffraction in coal-based graphitic carbons.* Carbon, 1996. 34(10): p. 1259-1265.

AUTHORS' ADDRESSES
Cagri Ayranci, PhD
Samira Aslanzadeh, PhD
Behzad Ahvazi, PhD
Yaman Boluk, PhD
University of Alberta
Mechanical Engineering Department
10-360 Donadeo Innovation
Centre for Engineering
9211 116 Street NW
Edmonton, Alberta, Canada T6G 1H9
CANADA